

Chapter 1

Designing Composite Wind Turbine Blades from Cradle to Cradle

Brahim Attaf

Expert/Researcher in Composite Materials & Structures
39 Blvd. Charles Moretti, 13014 Marseille - France
b.attaf@wanadoo.fr

I. INTRODUCTION

There is no doubt that the use of renewable energies is a positive answer in response to environmental and societal challenges that are facing our society nowadays. It is in this context that wind power is considered to be an alternative source of clean, green, eco-friendly and sustainable energy. To better identify the environmental issues, mitigate the adverse consequences of the greenhouse effect (GHE), minimize their impacts and understand the importance of the use of wind energy as a key feature to fight against global warming, it is worthwhile to address, in the introduction of this chapter, some preliminary points making the reader familiar with the GHE and the associated disequilibrium mechanism. On the other hand, the survey will concentrate on the design process of three-bladed horizontal-axis wind turbines (HAWTs).

A. Greenhouse Phenomenon and Radiative Balance

It is well known that the Earth receives energy from the Sun in the form of visible light called “solar rays” and about 30% of this energy is reflected by white clouds, ice, snow and lower atmosphere. On the other hand, 70% of the remaining energy is absorbed at the Earth’s surface by oceans, land and various components of the upper atmosphere. As a result, the absorbed energy heats the surface of the earth, and when the Earth’s surface becomes warm it radiates its own rays of heat called “infrared rays” (IR). The energy emitted is equivalent to the energy absorbed according to the principle of energy conservation.

As a matter of fact, climate scientists have revealed that in the absence of GHE, the average temperature of Earth’s surface would be $-18\text{ }^{\circ}\text{C}$ (Fig. 1a); and under such temperature conditions, life would be virtually impossible. However, in the presence of GHE, the temperature is about $+15\text{ }^{\circ}\text{C}$ (Fig. 1b). It is this temperature condition which enables human beings to live on the Earth’s surface. Furthermore, it was claimed that deregulation of Earth’s surface average temperature may be avoided if the value of $33\text{ }^{\circ}\text{C}$ which corresponds to the temperature difference between absence and presence of greenhouse gases (i.e., $+15\text{ }^{\circ}\text{C} - (-18\text{ }^{\circ}\text{C}) = 33\text{ }^{\circ}\text{C}$) is kept constant.

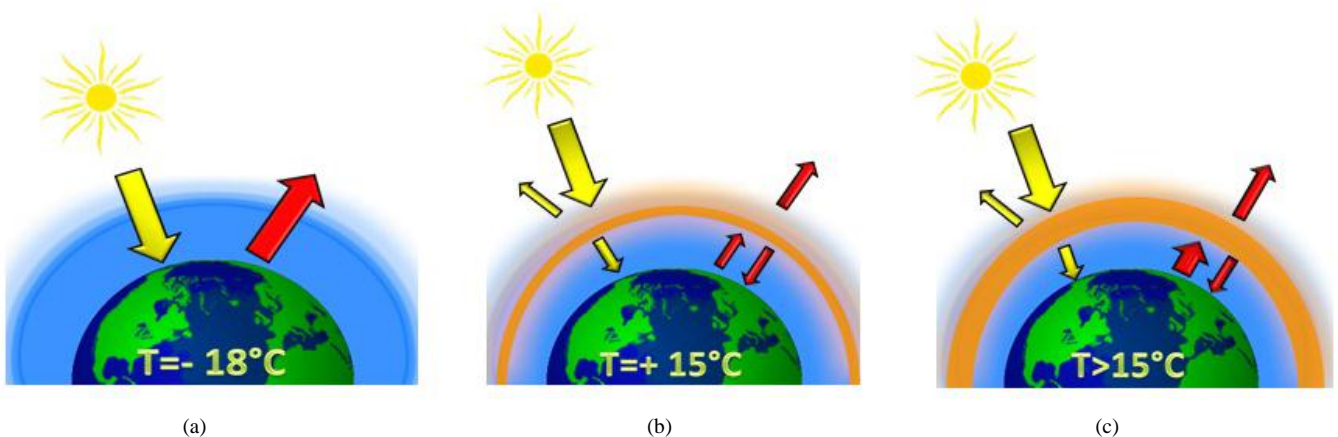


Fig. 1 Greenhouse effect (GHE): (a) in absence of GHE; (b) in presence of GHE; (c) disequilibrium of the greenhouse mechanism

However, human activities which are classified as industrial, agricultural and domestic have induced an increase in concentration of greenhouse gas (GHG) emissions in the atmosphere [1], where carbon dioxide (CO_2) is the main GHG produced by the human activity; it occupies 74% of the total GHGs. Fig. 2a illustrates the evolution of CO_2 concentration in the atmosphere over the last hundred and thirty years. This increase in temperature may lead to disequilibrium of the

greenhouse mechanism, which can cause global warming, because the Earth's surface temperature will be above +15°C. This increase in temperature can lead to a subsequent climate crisis for future generations (Fig. 2b).

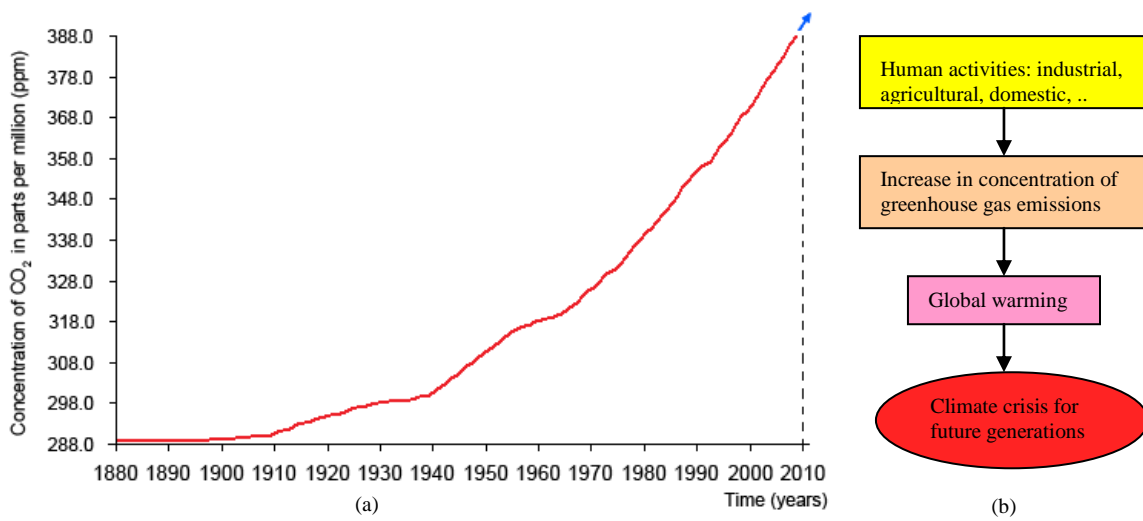


Fig. 2 Global warming: (a) concentration of CO₂ in the atmosphere vs time in years, (b) climate change and its consequences

Thus, the consequences of global warming can pose a catastrophic threat to human health and the environment. For instance, by 2100 the temperature across the globe could rise by 1.8 to 6 °C according to the agreements of experts and IPCC (Intergovernmental Panel on Climate Change) assessment reports [2, 3]. This increase in temperature will have dramatic impacts with notably:

- an increase in the sea level (15 to 95 cm);
- an effect on both drought and water resources;
- changes in rainfall and wind patterns (heavy rains, cyclones, hurricanes, tornadoes ...);
- an increase in tropical diseases such as malaria in some countries;
- ...

To address this problem and prevent global warming to rise, the only way is to reduce GHG emissions through the use of renewable energies: an important feature of the sustainable development concept.

B. Onshore and Offshore Wind Energy as an Alternative

As revealed by concrete studies that wind energy is a key solution responding to the sustainable development challenges through tackling air pollution, GHG emissions and various industrial wastes, the technological interest to develop larger and more powerful machines is becoming nowadays a major concern for worldwide wind turbine manufacturers [4, 5]. Depending on the statistical distribution of wind speed on the site, two classes of three-bladed HAWTs are considered today to be the most widely used turbines; these are the ones installed on land (i.e., onshore) and the ones installed at sea (i.e., offshore). For the latter class and according to the seawater depth, offshore wind turbines foundations are varying from floating to resting on a reinforced concrete placed into the bottom side of the sea (see Fig. 3). In addition, it was estimated that an offshore production site, situated a few kilometres away from the coast, could produce 50% more energy than onshore site. Furthermore, offshore wind turbines can provide in average 5 to 10 MW, while onshore wind turbine energy production is limited to 3 MW.

Thereby obtaining a high power output depends mainly on the swept area of the rotating blades. Theoretically, the maximum recoverable power of a HWT is given by Betz's formula [6]:

$$P_{\max} = \frac{16}{27} \frac{1}{2} \rho S v^3 \quad (1a)$$

where, P_{\max} is the maximum power (W); ρ is the air density (kg.m⁻³); v is the wind speed (m.s⁻¹) and S is the swept area (m²).

Under normal atmospheric conditions of pressure ($P=1.01325$ bar) and temperature ($T=15$ °C), the density of dry air at sea level is approximately equal to 1.225 kg.m⁻³. With this approximation, Eq. (1a) becomes:

$$P_{\max} = 0.3629 S v^3 \quad (1b)$$

It can be discerned from Eq. (1b) that, for a minimum revolution per minute (RPM) and a given blade number, the power is a function of the swept area S if the wind speed v and the tip speed ratio ($TSR=v_{\text{tip speed}} / v_{\text{wind speed}}$) are kept constant. In other words, the power depends on the radius of the area swept by the blades, wherein the radius is no other than the length l of the

blade as shown in Fig. 4.

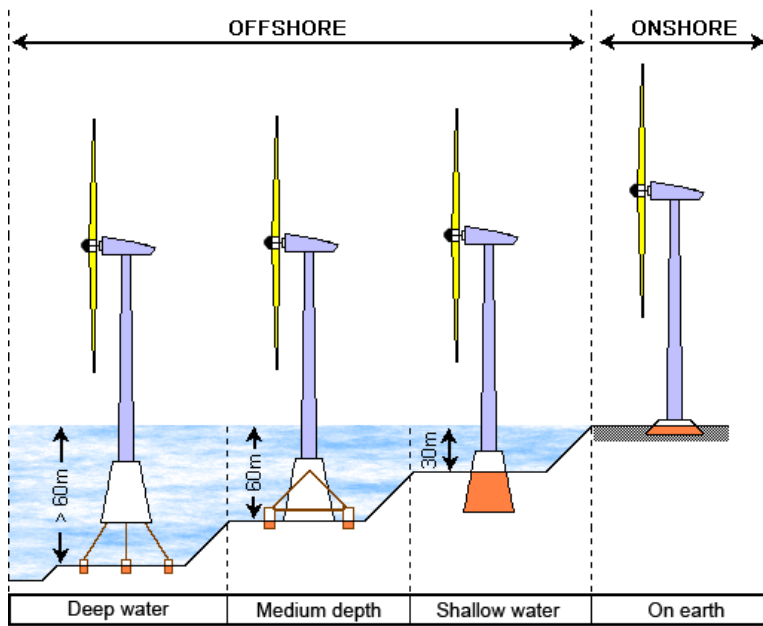


Fig. 3 Onshore and offshore horizontal-axis wind turbines

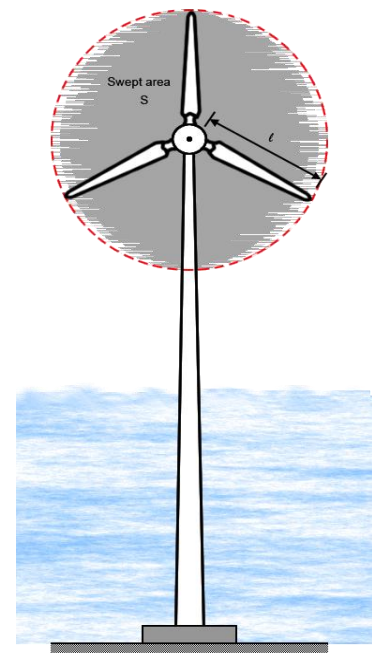


Fig. 4 Power output as a function of the blade length

In practice, this maximum power is multiplied by a coefficient of performance $C_p \in [0.2; 0.7]$, which depends on the type/model of the wind turbine and its installation site (offshore or onshore).

Further to that and under the conditions of constant v and TSR, it can be demonstrated from Eq. (1b) that the maximum power of a HAWT varies parabolically as function of the blade length: the larger the size of the blades, the more energy is captured.

Although the turbine blades rotate with a low speed, so they are less stressed, but this does not prevent them from exposure during their service life to static and dynamic loads, which may have negative effects on their structural behaviour and this may lead to risks of failure. Consequently, to overcome this problem and drastically reduce these risks, fibre-reinforced composite materials are widely used in the design and manufacture of these blades.

It is in this context that this chapter has been elaborated to present the different steps involved in the design process of wind turbine blades using composites based on long fibres and taking into account their optimisation in the manufacturing technology. The results and conclusions presented throughout this chapter can help wind industry designers to manufacture reliable blades capable to withstand, without any adverse effect, harsh environmental conditions and different types of possible shocks.

II. AIRFOIL GEOMETRY, BLADE DIMENSIONS, MATERIALS AND CHARACTERISATION

Although single- and two-bladed HAWTs offer a great saving in cost and weight, three-bladed HAWTs are the most widely used in the world because they offer a good visual impact, generate less noise and provide a better lifetime due to the rotor stability and the low rotation speed of blades. As the three blades are perfectly identical to each other, the analysis will focus only on a typical blade. This latter will be isolated from the whole system according to the substructure method with an accurate modelling of the boundary conditions.

A. Airfoil

The airfoil, or aerofoil, section is a slide of a wind turbine blade seen in cross-section; it is defined mainly by its leading edge, trailing edge, chord, maximum thickness and its associated location point. The important terms used to describe an airfoil are shown in Fig. 5. The airfoil shape is generally characterized by using the four-digit series developed by the National Advisory Committee for Aeronautics (NACA).

In collaboration with the specialized agencies in fluid mechanics and aerodynamics, the standardized profile of the blade can be designed and validated. On the other hand, to further increase the longitudinal blade stiffness, either a spar (box beam) or stiffeners (shear web) are incorporated into the internal structure; thus making the blade structure more stiff and resistant to wind loads and induced vibrations [7, 8]. The stiffeners can be located at 25% C and 55% C with regard to the blade leading edge, where the letter C denotes the chord of the considered airfoil. The upper and lower surfaces (i.e., skin of the blade) are both manufactured from fibre-reinforced laminates. Stiffeners are generally made of the same material that is used for upper

and lower laminated surfaces, but with different thickness.

The evolution of the twist angle (rotation of the profile with respect to the blade twist axis) from the blade inboard section to the blade tip can be improved by the competent bodies in the relevant research area. This twist angle is considered to be the reference for the setting angle for each section. However, the techno-scientific terminology between the position of the elastic centre and the centre of gravity must be the subject of a clear and precise distinction. Then comes the determination of the blade size that must meet a given specification, followed by the determination of different thicknesses, appropriate fibre orientations, and appropriate stacking sequences for each section. This step involves checking the blade mechanical strength using numerical methods.

B. Geometry and Dimensions

The number of zones for which the blade is divided is defined as a function of the blade length. Taking for instance the case of a blade of 8 m length, the structure thereof will be divided into four zones with variables thicknesses, thus four material zones are to be considered, and each material is affected to the corresponding zone. In addition and according to stress distributions along the blade length, a decrease in thickness ranging from blade root to blade tip has to be considered for each zone. In addition, a fifth material zone has to be considered for the two internal stiffeners; each stiffener has a thickness of 3 mm. The different material zones and their positions with regard to the blade structure are illustrated in Fig. 6; these are defined as follows:

- **Zone A:** upper or lower surface thickness = 12 mm
- **Zone B:** upper or lower surface thickness = 9 mm
- **Zone C:** upper or lower surface thickness = 6 mm
- **Zone D:** upper or lower surface thickness = 3 mm

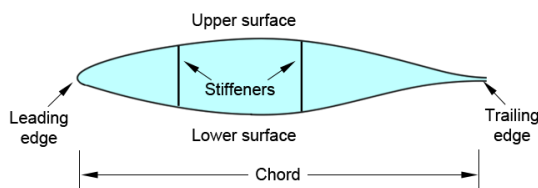


Fig. 5 Airfoil-shaped cross section

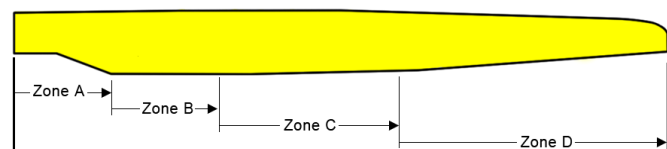


Fig. 6 Different thicknesses associated to different zones along the blade structure

C. Materials

1) Composite materials

Selected materials for the manufacture of wind turbine blades must meet, in one hand, the quality assurance requirements and, on the other hand, the new regulations related to environmental issues. To this end, it is very important to choose carefully: (i) the class of fibres, (ii) the class of matrix, (iii) the foam constituting the core of the sandwich (inserted into the section of the profile for small blades).

As the blade is an essential structural component within the wind turbine machine, it must therefore be designed structurally strong enough to support the various loads to which it may be exposed. In order to meet this requirement, glass-fibre composites such as glass-reinforced plastics (GRP) and carbon-fibre-reinforced plastics (CFRP) are suitable materials for use in such structural applications [9, 10] because of their excellent formability, their mass-saving advantage coupled with high stiffness and strength, and the greater freedom to tailor these high properties in the desired orientation and position. In addition, these lightweight materials have exceptional structural properties with precise objectives that cannot be achieved when using original or conventional materials. These attractive benefits have effectively opened up great opportunities in the design and manufacture of future wind turbine blades. In fact, many structural components of these blades, previously made from conventional materials, are now manufactured from composite materials and are operating successfully in their implantation sites.

2) Nanocomposites (carbon nanotubes)

According to recent advances in nanotechnology, it is expected that carbon nanotubes (CNTs) in the form of continuous fibres can be used in various structural applications and that in order to improve the material properties [11]. These nano-materials are based on graphite which is no other than the stable form of carbon at ordinary temperature and pressure (e.g., pencil tip, as shown in Fig. 7). Its molecular structure consists of an intercalated stacking of noncompact hexagonal honeycomb sheets; each sheet is separated by about 0.336 nm along its normal direction (see Fig. 8).

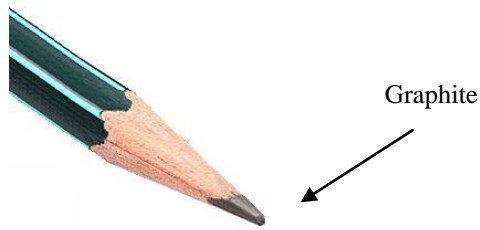


Fig. 7 Stable form of carbon (pencil tip)

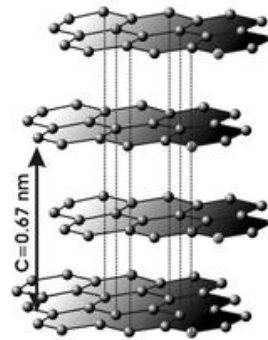


Fig. 8 Graphite molecular structure

Fig. 8 shows the molecular structure of graphene, i.e., a single flat layer of carbon atoms isolated from the crystal structure of graphite. The carbon nanotubes (CNTs) are obtained by rolling graphene sheets on themselves as shown in Fig. 9. Depending on the winding geometry, there are generally three types of CNTs, which are called: armchair, zigzag and chiral.

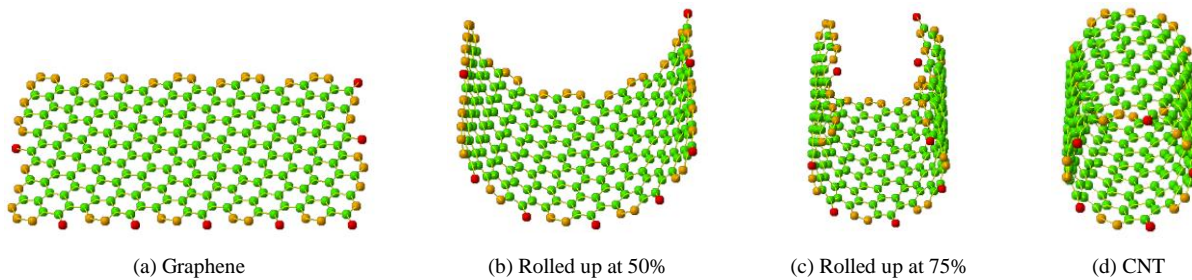


Fig. 9 Rolling up a graphene sheet into a carbon nanotube

In general, CNTs can be a single-walled carbon nanotube (SWNTs) as shown in Fig. 10a, or multi-walled carbon nanotubes (MWNTs) as shown in Fig. 10b. The diameter of CNTs is ranging from 1-80nm; whereas the length can reach several micrometres. With these nanometric dimensions, a very high aspect ratio (i.e., length-to-diameter) can be provided, however. Such unique characteristics contribute significantly to the improvement of the durability of structures and structural components.

For the production of CNTs, there are several processes, including the CVD (Chemical Vapour Deposition) process which has been achieved thanks to the recent development in the field of nanotechnology, where CNTs can be aligned in the same direction to form continuous fibres. The growth mechanism of CNTs using CVD process is shown in Fig. 11.

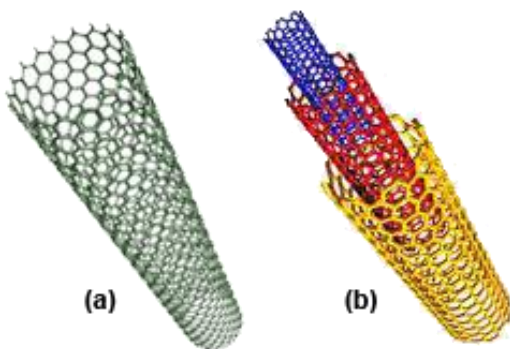


Fig. 10 Carbon nanotubes: (a) Single walled, (b) Multi-walled

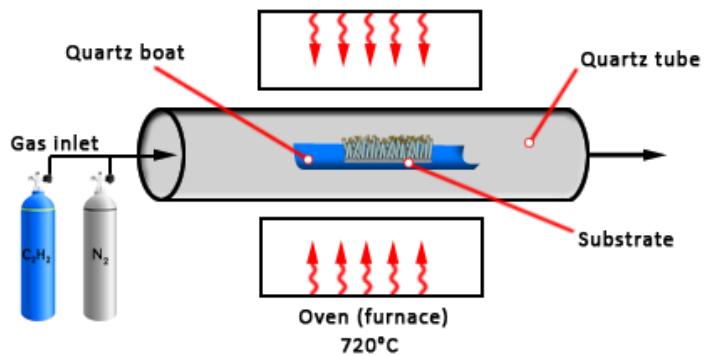


Fig. 11 CVD process for the production of CNTs

The main choice criteria of these nano-materials are believed to be related to the ultra-high-performance indices in terms of specific stiffness and specific strength and other physicochemical properties such as thermal and electrical conductivity. These advantages make CNTs attractive candidate for the reinforcement of composite materials that will play an important role in the design and manufacture of future structural blade parts.

In this fast-growing sector of research and innovation, several research activities are in progress with the object to build a new set of wind turbine blades. Significant improvements and challenges can be reached within the next generation of wind turbine blades made with carbon nanotube-based continuous fibres (see Fig. 12). For instance, the strength of these fibres can be several times higher than standard carbon fibres and weighs much less for an equivalent cross-section: an advantage that will provide a good solution to improve the overall mechanical behaviour of the blade.

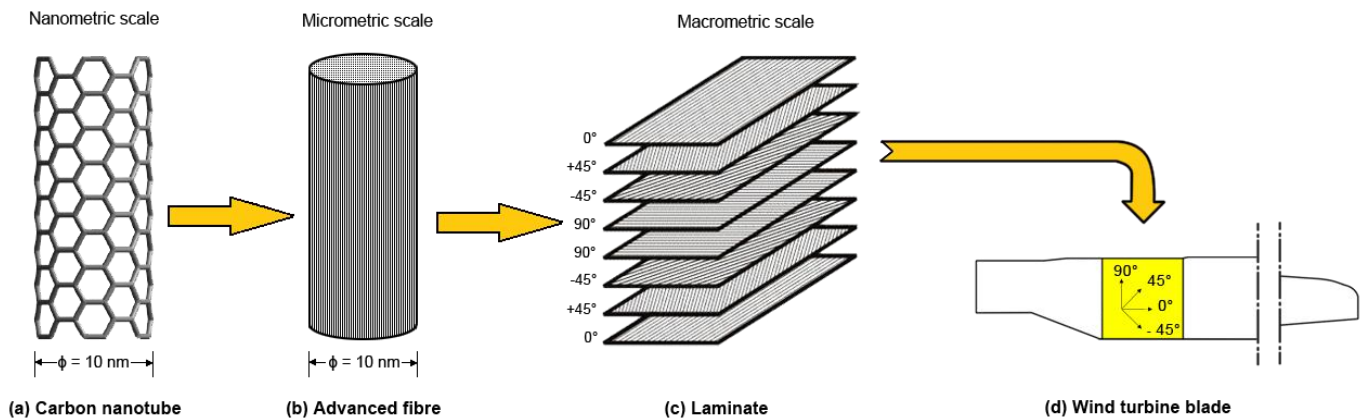


Fig. 12 Application of CNT-based continuous fibres for future design of ultra-mega wind turbine blades

With this great innovation, CNTs are likely to be exploited in the design and manufacture of wind turbine blades with ultra-length up to several hundred meters. This progress reflects the idea of building offshore wind turbines that are capable to produce ultra-mega sources of energy. In addition, CNTs have the potential to be used as sensors for monitoring the structural health of large wind turbine blades. However, from an ecological point of view, these materials are likely to have adverse impacts on the environment and human health throughout the entire cycle life [12].

D. Characterisation of Materials

In materials science, the properties necessary to describe the linear-elastic behaviour of selected fibre-reinforced composite plies can be predicted using the rule-of-mixture formulae, based on theoretical and semi-theoretical formulae. On the other hand, stress-strain curves are made to provide experimentally some of these properties according to standards that are available, such as ISO (International Standards Organization) and ASTM (American Society for Testing and Materials). Further to that, a correlation “calculation-test” is performed to improve the approach of the theoretical models. The necessary characteristics to carry out research activities can be physical, mechanical or hygrothermal.

1) *Physical characterization: it involves determining the following constants:*

- the fibre volume fraction, V_f (composites used in wind industry have a V_f varying between 40% and 60%);
- the fibre mass fraction, M_f (this terminology is less used than V_f);
- the ply thickness, t (it depends on the ply type and can be unidirectional, bidirectional or mat);
- the density, ρ (in other terms, the mass per unit volume).

2) *Mechanical characterization: it involves determining the following engineering constants:*

- Young's moduli in i -direction, E_i ($i=1, 2, 3$): a measure of material stiffness;
- Shear moduli in the i - j plane, G_{ij} (i - $j=2$ - $3, 3$ - 1 and 1 - 2): a measure of material stiffness;
- Poisson's ratio for transverse strain in the j -direction when stressed in the i -direction, ν_{ij} (vice versa ν_{ji});
- Tensile or compressive strength failure in i -direction, $\sigma_{i,f}$ ($i=1, 2, 3$): a measure of material strength;
- Shear strength failure in the i - j plane, $\tau_{ij,t}$ (i - $j=2$ - $3, 3$ - 1 and 1 - 2): a measure of material strength.

3) *Hygrothermal characterization: it involves determining the following hygrothermal expansion coefficients:*

- the thermal expansion coefficients, α_i ($i=1, 2, 3$);
- the moisture expansion coefficients, β_i ($i=1, 2, 3$).

In structural design, one of the key features that characterise the choice of materials are believed to be related to specific strength and specific stiffness; they are defined as the stiffness-to-weight ratio (E/ρ) and strength-to-weight ratio (σ_f/ρ), respectively. These two technical terms are distinct and their use in engineering design process must not be confused; they are both dependent on material type and its density. The advantage of composite materials is that they offer highest values of these ratios which, from mechanical and economic point of view, are very important because they meet specific needs required in vibration and stability analyses of wind turbine blades. The optimization of natural frequencies and critical buckling loads can be achieved through the selection of optimum ratios. Fig. 13 shows a comparison of specific strength and specific stiffness for some conventional, composite and nanocomposite materials [13, 14]. Within the composite family, it is easy to discern the position of glass-fibre reinforced polymer (GFRP), carbon-fibre reinforced polymer (CFRP) and carbon nanotubes (CNTs).

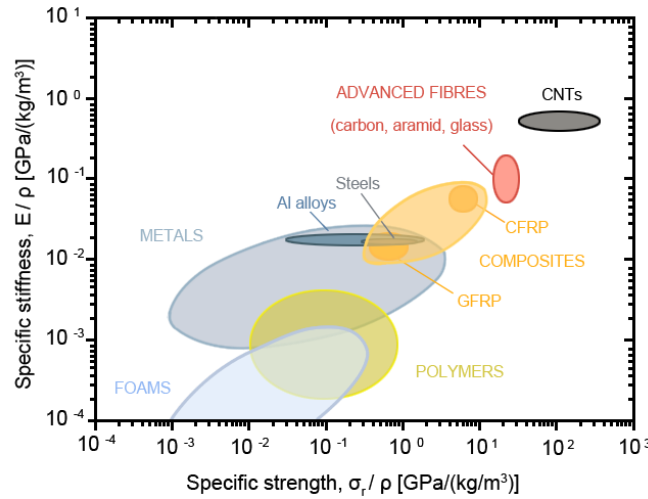


Fig. 13 Specific stiffness versus specific strength for some composite materials [13, 14]

III. FINITE ELEMENT ANALYSIS AND EXPERIMENTAL TESTING

The design of composite wind turbine blades must fulfil the normative requirements requested by the standards ISO 2394 and IEC 61400-1 in terms of structural analysis (stress, strength, vibration, fatigue, safety...) and static/dynamic tests of qualification. For the section relative to experimental analysis, it is assumed that the blade is already manufactured by the pre-selected process.

A. State of the Problem and Constitutive Equations

The state of the structural problem is illustrated in Fig. 14, where the blade structure (onshore or offshore) is assumed to be subjected to three main types of loading; these are: (i) mechanical loading (high wind forces, weight, ..), (ii) thermal loading (temperature variation) and (iii) hygrometric loading (moisture and seawater exposure) [15, 16].

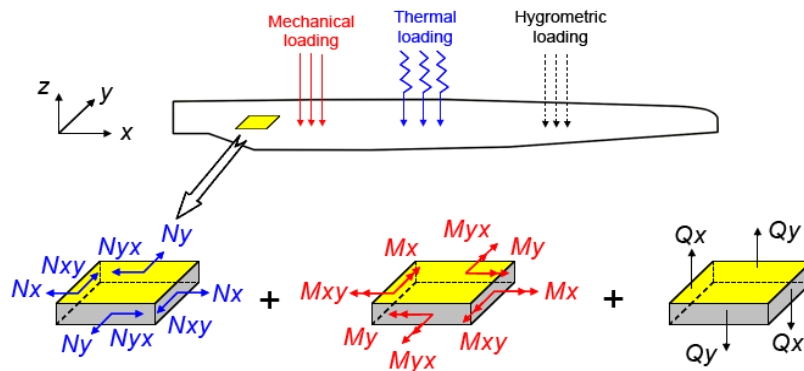


Fig. 14 Resultant forces and moments for a typical blade element subjected to hygrothermomechanical loading

When thermal and moisture effects besides mechanical loading are taken into consideration in the structural analysis, the constitutive relations for an unsymmetrically n -layered composite plate, assumed to be extracted from the blade structure, with transverse shear deformations (transverse hydrothermal effect is neglected) can be written in compact matrix form as [17, 18]:

$$\begin{Bmatrix} N \\ \dots \\ M \end{Bmatrix}_{xyz} = \begin{bmatrix} A_{ij} & B_{ij} \\ \dots & \dots \\ B_{ij} & D_{ij} \end{bmatrix} \begin{Bmatrix} \varepsilon_0 \\ \dots \\ \kappa \end{Bmatrix}_{xyz} - \begin{Bmatrix} N^{\Delta T} \\ \dots \\ M^{\Delta T} \end{Bmatrix}_{xyz} - \begin{Bmatrix} N^{\Delta m} \\ \dots \\ M^{\Delta m} \end{Bmatrix}_{xyz} \quad (2a)$$

$$\{Q\}_{xyz} = \{F_{ij}\} \{\gamma\}_{xyz} \quad (2b)$$

$$(A_{ij}, B_{ij}, D_{ij}) = \sum_{k=1}^n \int_{z_{k-1}}^{z_k} (\bar{Q}_{ij})_k (1, z, z^2) dz \quad (i,j=1,2,6)$$

$$F_{ij} = \delta_{ij} \sum_{k=1}^n \int_{z_{k-1}}^{z_k} (\bar{Q}_{ij})_k dz, \quad (i,j=4,5)$$

where, N is the in-plane forces vector; M is the bending/torsional moments vector; Q is the out-of-plane forces vector; ε^0 is the mid-plane strains vector; κ is the curvatures vector; γ is the transverse shear strain vector; A_{ij} is the extensional stiffness matrix; B_{ij} is the coupling stiffness matrix; D_{ij} is the bending stiffness matrix; F_{ij} is the transverse shear stiffness matrix; ΔT and Δm represent the variations of temperature and moisture, respectively. Whereas $(\bar{Q}_{ij})_k$ is the k -th ply stiffness matrix and δ_{ij} is the transverse shear correction factor.

Difficulties inherent to transverse shear deformation, anisotropy of material, blade geometry and boundary conditions constitute a complex and tedious analysis, which makes it impossible to provide a mathematical solution. To overcome these difficulties, numerical solutions using finite element method (FEM) and experimental investigations are the only approaches that can be employed.

B. Finite Element Analysis

A rigorous calculation of a wind turbine blade structure is generally complex. It may be interesting to obtain rapidly some estimated results for a simplified blade model using analytical formulations. However, for better approach the analysis becomes complicated and the analytical formulations may not provide acceptable results for use in practice. In such situation, the finite element method (FEM) is one of the numerical methods that can provide approximate solutions making then the process of optimum design easily achieved. The derivation of the FE formulations is out of scope for this analysis. However, theories and fundamentals related to the FEM can be found in [19, 20]. It should be pointed out, however, that due to the complex shape of the blade, the anisotropy of the material, the type of applied loads and the degree of accuracy, the elaboration of a numerical model of the blade-structure becomes a complex task, where the solution by the FEM turns into a difficult undertaking work.

For this purpose, a validated commercial finite element computer program can be used to perform analyses of the blade structural behaviour when subjected to static and dynamic loading conditions. To this end, the physical model can be divided longitudinally, transversely and vertically (for stiffeners) into a large number of elements.

Since the elements type choice, used for the discretisation of the different components constituting the whole blade-structure, has a significant influence on the output results, the selected element must be representative and consistent with the real case. For instance, the four-node 12-DOF (degrees of freedom) rectangular plate bending element (see Fig. 15) can be used to create a mesh for the upper and lower blade surfaces; each node possesses six independent degrees of freedom: three displacements u , v , w and three rotations θ_x , θ_y , θ_z . However in most cases of analysis, the rotation around the z -axis θ_z is neglected. On the other hand, the points of attachment of the blade root to the turbine rotor are modelled as fully clamped boundary conditions.

Once the numerical results are obtained, their analysis reveals that further means of strengthening the blade structure still needed to be applied. This requirement is achieved through a reinforcement of the internal section of the blade (i.e., airfoil) with longitudinal stiffeners or box beam structures. Under these conditions, a preliminary study should be undertaken to determine the appropriate number of stiffeners and their position with respect to leading edge. In this context, [21, 22] have developed some interesting results that may be exploited by the wind turbine industry, showing the possibility to reduce the maximum displacement of a composite plate without introducing weight penalty by the incorporation of one, two or three stiffeners as a structural reinforcing elements.

Further numerical results on the blade structural behaviour show that areas with irregular geometrical changes, characterised generally by the shift from a circular shape to airfoil shape, reveals the presence of stress concentration at the transition zone. Therefore, a particular study must be undertaken on the highly stressed areas, and this in order to check the condition of non-failure of individual plies. For this purpose, several criteria of ply failure have been developed and are available in composite materials literature, namely: Tsai-Hill, Tsai-Wu and Hoffman criteria.

For instance, the Tsai-Hill failure criterion function in the state of plane stress (i.e., $\sigma_3 = \tau_{13} = \tau_{23} = 0$) is given for each ply constituting the laminate by the following Eqs. [17, 18]:

$$\left(\frac{\sigma_1}{X}\right)_{(k)}^2 + \left(\frac{\sigma_2}{Y}\right)_{(k)}^2 - \left(\frac{\sigma_1 \sigma_2}{X^2}\right)_{(k)} + \left(\frac{\tau_{12}}{S}\right)_{(k)}^2 < 1 \quad (3)$$

where, X is the maximum tensile (compressive) failure stress in the 1-direction, Y is the maximum tensile (compressive) failure stress in the 2-direction and S is the maximum shear failure stress in the 1-2 plane.

Fig. 16 illustrates an example of stress concentration for static analysis of a typical ply composing the laminate blade within the transition zone. Failure plies are those for which the failure criterion function, described by Eq. (3), is greater than the limit value of 1 (i.e., 100%).

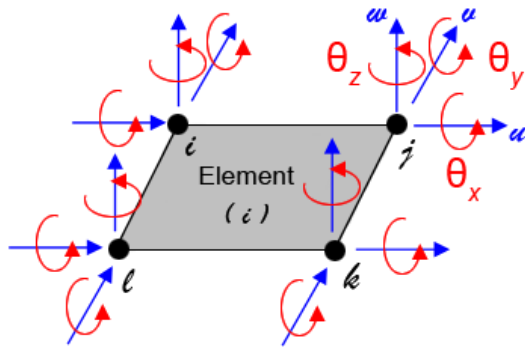


Fig. 15 Four-node 12-DOF rectangular plate bending element

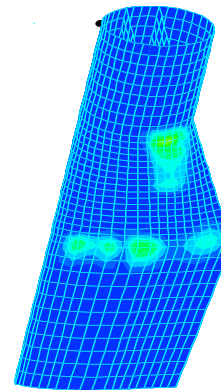


Fig. 16 Stress concentration in the transition zone for the k -th ply

By applying the Tsai-Hill criterion for the case of 8 m blade length when this latter is subjected to mechanical loading, it was found that the highly stressed ply is located within the transition zone, and the maximum value of the failure criterion function was found to be approximately equal to 85%. Whereas for the case of 24 m blade length, calculations show that the value corresponding to the highly stresses ply exceeds 100% (the concerned area is generally highlighted in red). In order to remedy this situation and avoid such failure prediction from happening, the ply initially made of glass fibre was replaced by another ply made of carbon fibre. In such case, the problem of structural analysis becomes complex because it deals now with the case of hybrid composite wind turbine blade made of two types of fibre reinforcements: glass and carbon.

In order to get a comprehensive understanding on the structural behaviour of the 8 m composite blade structure under free vibration, the modal analysis was performed using FEM computer programme and the numerical results of natural frequencies and mode shapes are plotted and presented in Fig. 17.

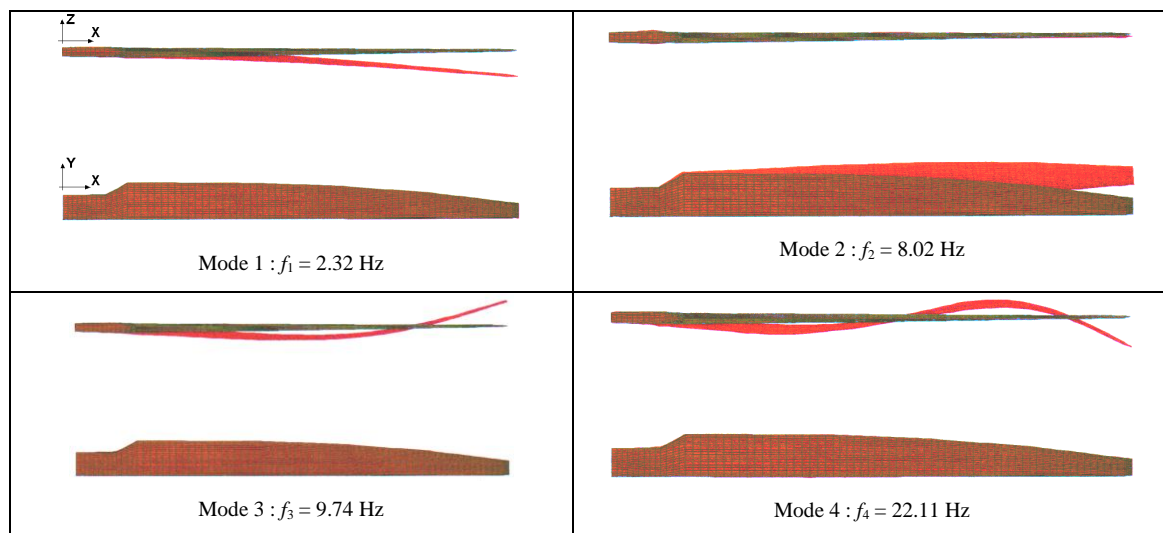


Fig. 17 First four numerical natural frequencies and associated mode shapes of a composite wind turbine blade (8 m length)

The natural frequencies which lie within the frequency range of application must be shifted beyond the forcing frequencies and this in order to avoid resonance phenomenon. The mode shapes give an idea about the deflected shape of the blade structure under each natural frequency and this information can help designers to locate the areas of high amplitudes, where fibre type and orientation could be tailored to reduce these amplitudes. For instance, incorporating fibres with high stiffness-to-weight ratio (E/ρ) can reduce the large amplitudes of vibration and lead to an increase of the natural frequencies.

C. Experimental Analysis

In compliance with the strict condition of the sub-structuring method, the boundary conditions that are representative of the real turbine blade fixture (i.e. attachment of the border blade root to the rotor system) were performed by a mechanical fastening system. It consists of fixing the turbine blade root between two circular steel frames with forty HR bolts (high strength friction grid bolts). The whole system was then mounted on a strong and stiff steel frame.

1) Static testing

For the static test, the prediction of the ultimate load that the blade is expected to withstand is performed using an inextensible cable placed at a specific location (i.e., center of aerodynamic loads in the case of small blades). The tensile force

applied to the cable represents a simulation of the resultant wind forces, the weight of the blade and eventually other loads resulting from environmental conditions. In order to avoid stress concentration and allow the applied load to be uniformly distributed over the defined location without risk of damaging the gel coat layer, a wooden system, known as a saddle, is mounted on that location; it is perfectly cut to match the geometric shape of the blade profile at the considered section. For large blades, the system remains the same but this time is performed with several saddles positioned on different locations along the blade. It should be noted, however, that old methods and contemporary techniques can be used to predict the blade maximum bearing load, namely: sandbags, hydraulic actuators, electrical winches, ...

2) *Dynamic testing*

For the free vibration analysis (modal analysis), the blade is subjected to a series of base load excitation. However, the vibration data analysis of the input (impulse force) and the output (acceleration response) in the time history does not give much information for engineering purposes. Therefore, a transformation from the time domain to the frequency domain is necessary and provides the results of spectral analysis of the original time history in the form of an amplitude-frequency spectrum via the Fast Fourier Transform (FFT) technique [21]. For this purpose, an impact hammer can be utilised to obtain the blade natural frequencies, whereas a shaker can be used to demonstrate the mode shapes of vibration.

(a) For the **impact testing**, a hammer (B&K) is used to excite the blade structure via a force transducer mounted on its head. To enable the impact to be reduced but more energy to be produced to excite the whole blade structure without damage or without introducing non-linear responses, an interchangeable resilient material (rubber or plastic) can be attached to the hammer tip. The time histories of the impulse force and acceleration in the form of signals are digitally sampled and stored in a multi-channel digital recorder and controlled by a digital signal processing software which is mounted on a computer. The lower modes of resonance can be detected using a piezoelectric accelerometer strategically placed on the blade structure.

(b) For the **shaker testing**, the measurement is based on the swept frequency method. The electromagnetic shaker is suspended using elastic system and connected to the load cell through a slender rod called stringer, to allow the blade structure to move freely in the other directions (see Fig. 18). The slender rod has a strong axial stiffness, but weak bending and shear stiffness. Consequently, it carries only axial loads but negligible moments or shear loads. To excite the resonant frequencies of a large blade, the size of the shaker is proportional to the size of the blade.

(c) For the **no-contact testing**, modal testing and vibration measurements have evolved over time. For the prediction of the blade natural frequencies and associated mode shapes, the no-contact measuring devices such as the technique of laser Doppler vibrometry (LDV) are highly used because they offer several advantages over the contact measuring systems, namely in terms of high measurement resolution, no calibration of accelerometers, low hysteresis loop, no risk of damaging the blade skin, ...

(d) For the **mode shape demonstration**, it is necessary to measure at each resonant frequency of the blade (i) the displacement amplitude at a sufficient number of points and (ii) the corresponding phase relationship between these points. The number of accelerometers and their location on the blade depend on the mode shape to be measured. A vibration pick-up for several points on the blade can be made and the motion of each accelerometer is recorded. Another pick-up (shaker), held at fixed point on the blade, provides a signal used as phase reference, to determine whether the blade motion at various points is in phase or out of phase with the input. And by connecting the points of different amplitudes at the same resonant frequency, the corresponding mode shape can be traced out (Fig. 19). For the higher modes, this method tends to be too complex to distinguish the mode shapes. Consequently, a large number of accelerometers are required.

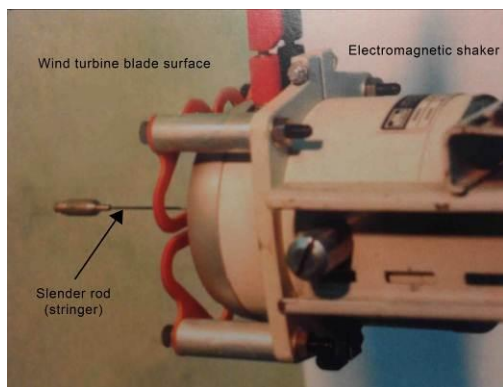


Fig. 18 Electromagnetic shaker load cell and slender rod (stringer)

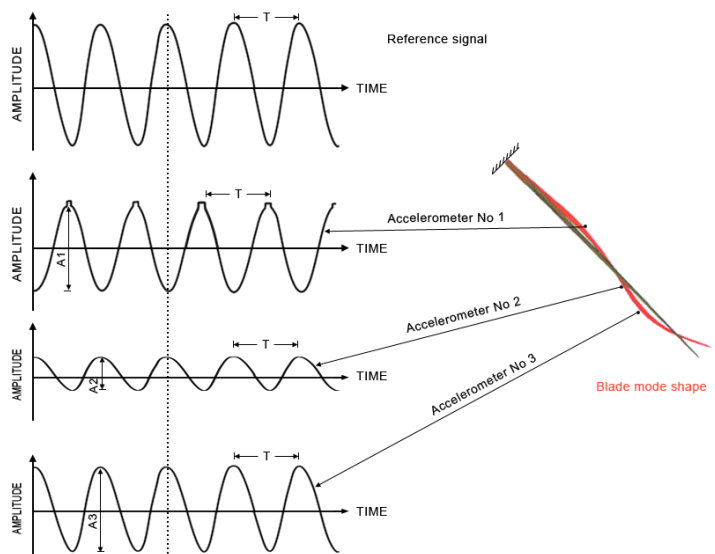


Fig. 19 Demonstration of mode shapes by the method of accelerometers

A typical magnitude against frequency relationship for the 8m composite blade is shown in Fig. 20. Each resonant frequency has a peak value corresponding to the natural frequency of that mode. As can be seen from Fig. 20, strong frequency components are noted at 2.5Hz, 10.5Hz, 23.50Hz and 40.13Hz, which are the fundamental and the three bending modes, respectively.

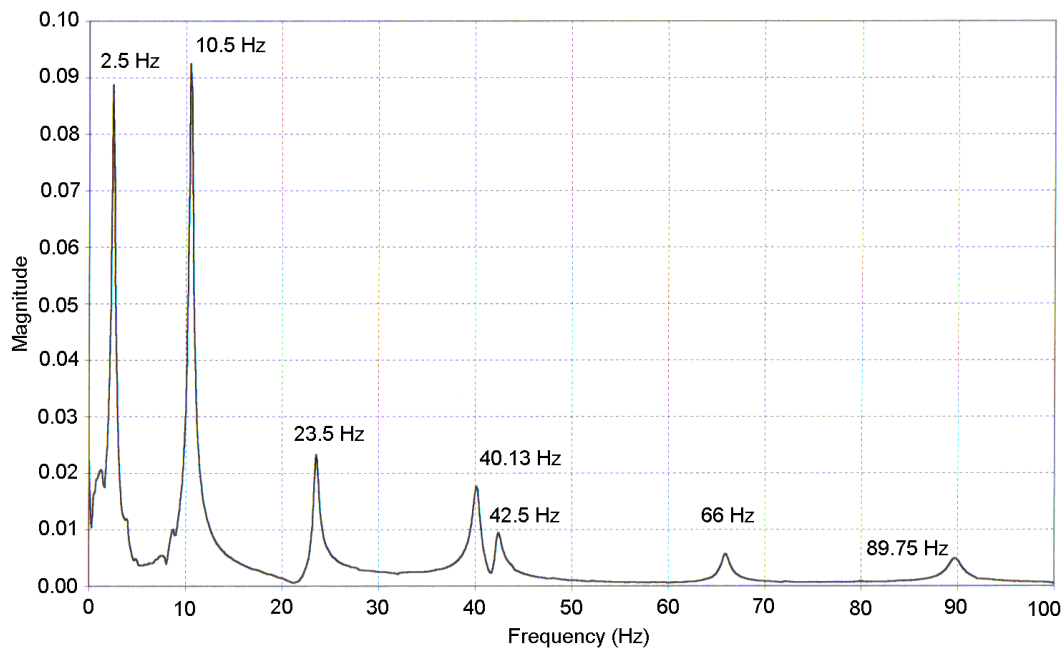


Fig. 20 FFT spectrum of clamped composite wind turbine blade (8 m)

Once the experimental and numerical structural analyses of the wind turbine blade are performed, a comparative study should be undertaken between experimental and numerical results. This correlation “test-calculation” is carried out in order to correct the numerical finite element model and determine whether the basic assumptions made on the material properties, the type of loading and boundary conditions have been properly modelled. When the correlation is good, the numerical model is accepted and validated. Then, an optimisation procedure can be initiated on the basis of the numerical model. This will save considerable time and money during the design process.

For instance, numerical and experimental natural frequency results for the 8 m composite blade are recapitulated in Table 1. It can be observed that there is a non-monotonic frequency sequence between both techniques (i.e., experimental and numerical); for some modes the natural frequencies are higher and for other modes are lower than the finite element values. The source of these variations is believed to be associated to (i) the variation in thickness of the lower/upper surfaces and internal stiffeners of the blade; and/or to (ii) the variation of the material properties. This source of discrepancies can be related to the process of manufacturing. However, a correlation between the two results shows that the percentage error between the two analyses is less than 10%: a value that is generally accepted in practice.

Further to that, it should be noted from Table 1 that the drag mode (i.e., mode 2) does not appear in the experimental results illustrated by the FFT spectrum shown in Fig. 20; this is due to the position of the accelerometer and the direction of the excitation force. For that mode, the accelerometer behaves in the same way as if placed on a nodal point (i.e., zero amplitude). In such situation, the considered mode is not detected at that position.

TABLE 1 NUMERICAL AND EXPERIMENTAL NATURAL FREQUENCIES OF 8 M COMPOSITE WIND TURBINE BLADE

Mode number	Natural frequency (Hz)	Mode description
1	2.62 (2.50)	Bending mode
2	9.53 (----)	Drag mode
3	11.17 (10.50)	Bending mode
4	24.26 (23.50)	Bending mode
5	39.36 (40.13)	Bending mode
6	43.06 (42.50)	Bending mode
7	68.24 (66.00)	Torsional mode

(---) Parenthesized values denote experimental frequencies

D. Concluding Remarks

The use of finite element method constitutes an appropriate technique providing better approach for examination of the blade behaviour under static and dynamic conditions. The output results are obtained at low computational cost, which provides a significant advantage for optimal design analysis. In applying this technique, the significant factors influencing the static and dynamic structural behaviour are analysed and optimisation studies can be made to arrive at an adequate blade structure that fulfils an efficient structural performance coupled with an economic design. Static and dynamic analyses will provide a better understanding of the structural behaviour of the composite wind turbine blade and will determine the high stressed plies and areas with high structural deflection which are likely to yield a risk of damage.

To avoid stress concentration, resonance phenomenon as well as fatigue problems, one or a combination of the following solutions may be involved during early design development:

- minimization of the maximum structural deflections by incorporating longitudinal stiffeners without introducing significant weight penalty;
- reduction of high amplitudes by placing fibres in the most effective direction;
- minimization of high amplitudes by selecting the appropriate laminate stacking sequence;
- optimisation of the natural frequencies via composite materials that exhibit high stiffness-to-weight ratio;
- reduction of the vibration amplitudes by choosing resin matrix exhibiting high viscoelastic damping.

A comprehensive modelling of a finite element solution from an experimental procedure should be undertaken before parameter studies are made. This will ensure a reliable design, allowing the blade structure to operate safely under severe static and dynamic conditions within the application range of loading and forcing frequencies.

IV. MANUFACTURING PROCESSES AND FORMULATION OF THE PERMEABILITY

A. Manufacturing Processes

In the wind turbine industry, commonly three-bladed turbine, each composite blade can be manufactured using either open mould (e.g., hand lay-up, spray-up) or closed mould (e.g., infusion, resin transfer moulding = RTM for short). However, to respond positively to the new regulations put into force on manufacturing processes and control of VOC (volatile organic compound) emissions such as styrene vapours, it is imperative to use the technology of closed mould. This will indeed ensure the sustainability of the manufacturing process.

With this argument as an objective, two processes currently used for the production of composite wind turbine blades will be discussed in the next section of this chapter; these are: (i) the vacuum infusion process and (ii) the RTM process. However, particular attention and a significant interest will be given to the RTM process. The reason for this is that, in addition to the participation in the reduction of VOC emissions, the RTM process has an industrial solution for the production of wind turbine blades coupled with high quality finishing, good mechanical properties, lower cost, and a total absence of bonding operation of half shells.

1) Vacuum infusion process

The principle of this moulding process consists of applying firstly a release film on the inner face of the mould, followed by a thin layer of gel coat. Next, comes the application of dry fibre reinforcements over the coated area, followed by (i) a peel ply, (ii) a separator film and (iii) a breather. Finally, the whole system is enveloped in bagging film (air tight plastic film) as shown in Fig. 21. Thus, the plastic film will play the role of the top part of a standard mould and acts as a flexible support. Under these conditions, the vacuum created in the closed chamber allows the resin to spread and gradually impregnate the fibre reinforcements until saturation. Once the resin is cured, the plastic film, the peel ply, the separator film and the breather are removed and the upper or lower blade parts are easily demoulded using compressed air and plastic wedges acting as spacers. Before operating, specific locations are carefully defined to prevent any kind of scratches that may occur to the coated blade surface while using plastic wedges.

When applying this process, the composite blade structure is made from two half-shells (upper and lower skins) and a longitudinal spar reinforcement; where each structural part is moulded separately. Then, all the parts are bonded together with a bi-component adhesive (resin and hardener) for producing the full blade. Fig. 22 illustrates an airfoil cross-section of a wind turbine blade internally reinforced by either a box beam configuration or shear web (stiffeners) as shown in Figs. 22a and 22b, respectively. Areas where the adhesive is applied are highlighted in red. At these bonded areas, the transfer of loads from one structural component to another must be performed without any adverse effect that could damage the mechanical strength of the adhesive joint. In the design procedures, the adhesive joint must be designed strong enough to perform safely in operating conditions and hold up the maximum load bearing capacity, fatigue resistance and climate conditions. With these reactions in mind, the author has undertaken some research and development studies on the evolution of the shear stress through the adhesive joint length and the output results are presented and discussed elsewhere [23].

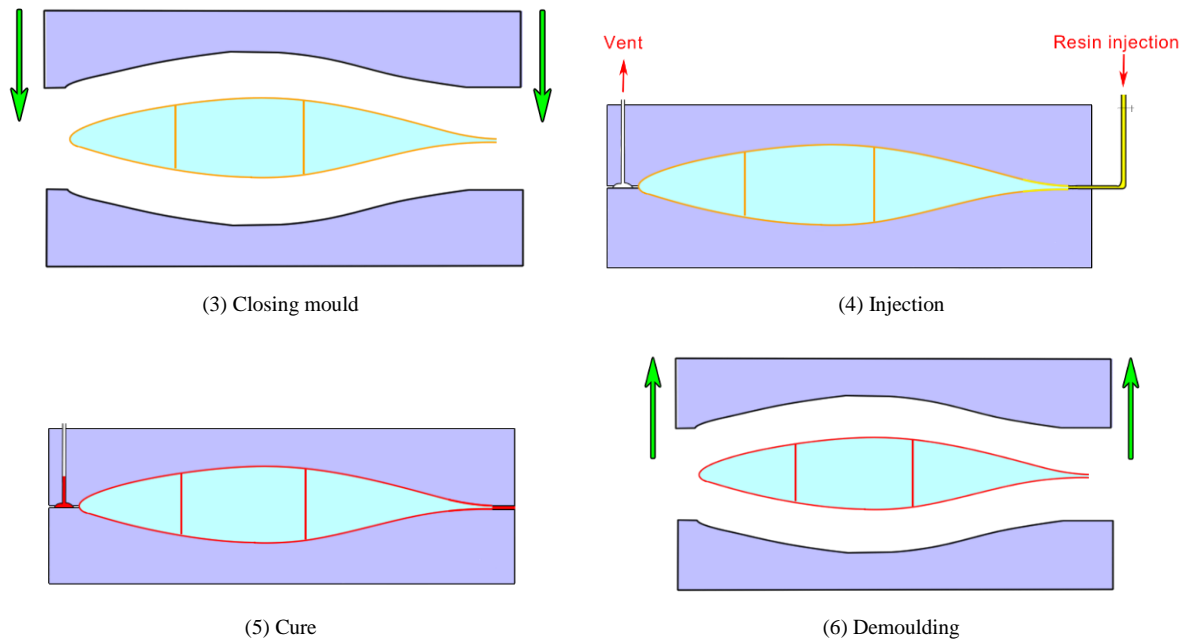


Fig. 23 Different stages for manufacturing a composite wind turbine blade by the RTM process

B. Formulation of the Permeability (Darcy’s law)

1) Method of measuring one dimensional permeability

In 1856, Henry Darcy [27] has shown that for a Newtonian incompressible fluid in laminar flow, the speed at which the fluid behaves in a homogeneous isotropic medium is proportional to the pressure gradient and inversely proportional to its dynamic viscosity.

To facilitate the comprehension of the relationship existing between the injection parameters, the analysis will first focus on the case of one-dimensional (1-D) permeability measurement for a simplified model of a wind turbine blade section, as illustrated in Fig. 24. However, it should be noted that the inner part reinforcing the blade structure (i.e., box beam or shear web) takes the form of the letter H, and thus, in order to avoid the risk of air entrapment.

From Darcy’s law considerations, the flow of resin Q through a cross-sectional area S can be expressed by:

$$Q = \frac{k}{\mu} \times S \times \frac{\Delta P}{\Delta L} \tag{4a}$$

Using the pressure gradient notation (i.e., $\nabla P = \Delta P / \Delta L$) leads to

$$Q = \frac{k}{\mu} \times S \times \nabla P \tag{4b}$$

where, Q is the flow rate ($\text{m}^3 \cdot \text{s}^{-1}$); S is the cross-sectional area to be impregnated (m^2); μ is the fluid viscosity ($\text{Pa} \cdot \text{s}$); ∇P is the pressure gradient ($\text{Pa} \cdot \text{m}^{-1}$) and k is the permeability (m^2).

The permeability k can be deduced from Eq. (4a), it is theoretically expressed by:

$$k = \frac{Q}{S} \times \frac{\Delta L}{\Delta P} \times \mu \tag{5a}$$

Furthermore, Darcy’s experience is based on the variation of the flow rate Q as a function of the pressure drop ΔP , as shown in Fig. 25. Thus, the permeability is defined experimentally by:

$$k = \frac{\mu \times \Delta L}{S} \times (\text{slope}) \tag{5b}$$

And after replacing in Eq. (5b) the slope by its value, deduced graphically from Fig. 25, the permeability k can easily be calculated for fixed values of μ , ΔL and S .

To get an estimate of the permeability magnitude k , let us consider the following values as an example: $\Delta L = 0.2 \text{ m}$; $S = 0.001 \text{ m}^2$; $\mu = 50 \times 10^6 \text{ Pa} \cdot \text{s}$; $\Delta P = 0.2 \times 10^6 \text{ Pa}$ and $Q = 2 \times 10^{-6} \text{ m}^3 \cdot \text{s}^{-1}$. Consequently, the application of Eq. (5) yields a value of permeability $k = 100 \times 10^{-12} \text{ m}^2$.

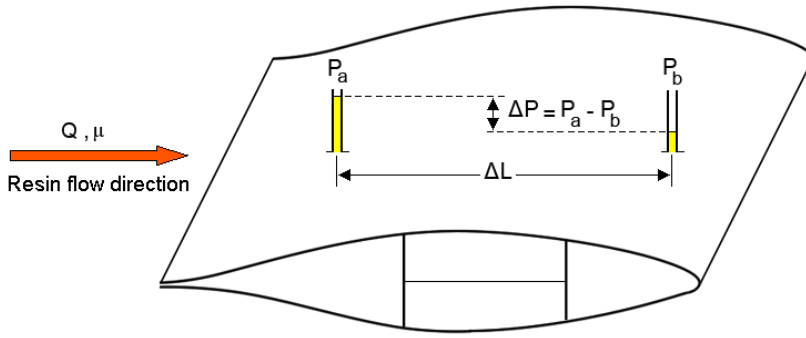


Fig. 24 Measurement of permeability by injection

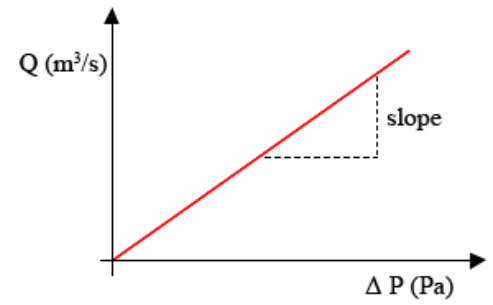


Fig. 25 Flow-pressure relationship

Dimensional study shows that in materials science, the permeability k is expressed in m^2 ; whereas in hydrogeology and oil/petroleum industries, this latter is expressed in Darcy ($1 \text{ Darcy} = 0.97 \times 10^{-12} \text{ m}^2$).

Furthermore, it should be noted that in some documentation there is sometimes confusion in terminology between *permeability* and *coefficient of permeability*. It is convenient to note these two parameters by the letters k and K , respectively. In this regard, the coefficient of permeability, K , is expressed in $(\text{m} \cdot \text{s}^{-1})$ and simply defined by the following ratio:

$$K = \frac{k}{\mu} \quad (6)$$

2) Longitudinal and transverse permeabilities

Eq. (4b) can be generalized in a three-dimensional (3-D) system, as illustrated in Fig. 26, where Darcy's law can be written in the following compact matrix form [29, 30]:

$$\{\bar{v}\} = -\frac{1}{\mu} [k] \{\nabla P\} \quad (7a)$$

or in the following developed matrix form:

$$\begin{Bmatrix} v_x \\ v_y \\ v_z \end{Bmatrix} = -\frac{1}{\mu} \begin{bmatrix} k_{xx} & k_{xy} & k_{xz} \\ k_{yx} & k_{yy} & k_{yz} \\ k_{zx} & k_{zy} & k_{zz} \end{bmatrix} \begin{Bmatrix} \partial P / \partial x \\ \partial P / \partial y \\ \partial P / \partial z \end{Bmatrix} \quad (7b)$$

where $\{\bar{v}\}$ is the velocity vector ($\text{m} \cdot \text{s}^{-1}$); $[k]$ is the permeability tensor (m^2); $\{\nabla P\}$ is the pressure-gradient vector ($\text{Pa} \cdot \text{m}^{-1}$).

Generally, the thicknesses of the laminate constituting the blade structure are thin in comparison with its other lateral dimensions (length and width). To this end, the transverse permeability through the preform thickness (along the z -axis) is very small in comparison to the other lateral permeabilities and may therefore be neglected ($k_{zx} = k_{zy} = k_{zz} = 0$). Based on this assumption, Eq. (7b) can be written in the two-dimensional flow system (2-D) as:

$$\begin{Bmatrix} v_x \\ v_y \end{Bmatrix} = -\frac{1}{\mu} \begin{bmatrix} k_{xx} & k_{xy} \\ k_{xy} & k_{yy} \end{bmatrix} \begin{Bmatrix} \partial P / \partial x \\ \partial P / \partial y \end{Bmatrix} \quad (7c)$$

As the permeability tensor $[k]$ depends on the angle of fibre orientation, θ ; it can therefore be written as [30]:

$$(i) \quad \text{in the } (1, 2) \text{ principal coordinate system: } \begin{bmatrix} k_{xx} & k_{xy} \\ k_{xy} & k_{yy} \end{bmatrix} = \begin{bmatrix} k_{11} & 0 \\ 0 & k_{22} \end{bmatrix}$$

$$(ii) \quad \text{in } (x, y) \text{ general coordinate system: } \begin{bmatrix} k_{xx} & k_{xy} \\ k_{xy} & k_{yy} \end{bmatrix} = \begin{bmatrix} k_{11}C^2 + k_{22}S^2 & (-k_{11} + k_{22})CS \\ (-k_{11} + k_{22})CS & k_{11}S^2 + k_{22}C^2 \end{bmatrix}$$

where, $C = \cos\theta$, $S = \sin\theta$

Also, the permeability in (1, 2) system can be evaluated from Carman-Kozeny Eq. [31] as follows:

$$k_{ij} = \frac{1}{c_{ij}} \frac{R_f^2}{4} \frac{(1 - V_f)^3}{V_f^2} \quad (i, j = 1, 2)$$

where c_{ij} is Kozeny constant, R_f is the fibre radius and V_f is the fibre volume fraction.

In the case of 3-D system flow, the average transverse permeability \bar{k}_{ij} for a preform composed of n plies can be calculated according to the rule of superposition:

$$\bar{k}_{ij} = \frac{1}{H} \sum_{k=1}^n h^{(k)} k_{ij}^{(k)} \tag{8}$$

where H is the total thickness of the preform and $h^{(k)}$ is the thickness of each ply k ($k= 1, 2, \dots, n$).

Using a combination of Darcy’s law and continuity equations yields the equation governing the pressure distribution, which can be written in compact matrix form as:

$$\nabla \cdot \left(\frac{[k]}{\mu} \{\nabla P\} \right) = 0 \tag{9a}$$

Or in fullydeveloped form, Eq. (9a) can be written as:

$$\frac{\partial}{\partial x} \left(\frac{k_{xx}}{\mu} \frac{\partial P}{\partial x} \right) + \frac{\partial}{\partial x} \left(\frac{k_{xy}}{\mu} \frac{\partial P}{\partial y} \right) + \frac{\partial}{\partial y} \left(\frac{k_{yx}}{\mu} \frac{\partial P}{\partial x} \right) + \frac{\partial}{\partial y} \left(\frac{k_{yy}}{\mu} \frac{\partial P}{\partial y} \right) = 0 \tag{9b}$$

This system of equations can be solved by numerical approaches for which the associated boundary conditions are appropriately defined [31].

For large-scale composite wind turbine blades, designed mainly for offshore applications, the resin injection is carried out in a sequential manner. In application of this technique, Fig. 27 shows the position of the injection and vent ports and illustrates how the injection process is performed. This latter starts from the blade root, defined by the section S_1 (transition zone), and once the fibrous preform corresponding to section S_1 is saturated with resin, the operation of injection is then moved progressively to the next section S_2 and so on, until the last section S_n is reached. This latter case corresponds here to the section covering the blade tip.

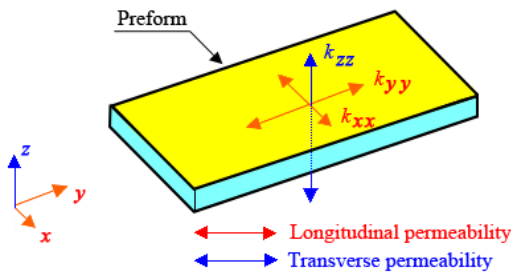


Fig. 26 Permeabilities in a 3-dimensional flow system

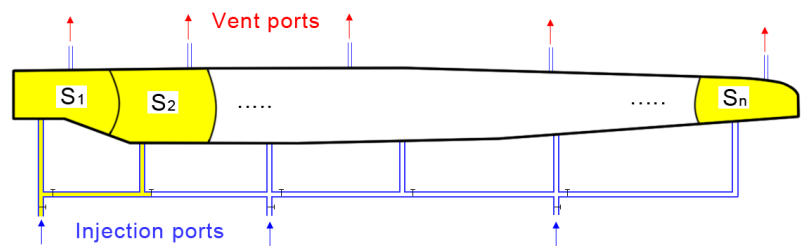


Fig. 27 Sequential injection for RTM process

C. Simulation of Flow Resin Behaviour for Composite Wind Turbine Blade Section

1) Case of orthotropic preforms

Three cases of lay-up constituting the orthotropic preforms were achieved by superposing several unidirectional plies, all orientated in the same angle θ ; these are: (i) lay-up at $[0^\circ]$, (ii) lay-up at $[90^\circ]$ and (iii) lay-up at $[45^\circ]$. Positions of injection and vent ports are illustrated in Fig. 28a-c. The angle $\theta=90^\circ$ is the reference angle which corresponds to fibres orientated along the length of the blade.

From Fig. 28a, it can be seen that the flow of the resin along the fibre direction $\theta=0^\circ$ is more important than the other directions (Figs. 28b and c). The reason for this is due to the presence of important volume fraction of pores in the longitudinal direction of fibres that are parallel to the direction of resin flow. Obviously, the presence of these pores will provide the preferential path of resin flow through the porous medium and will accelerate the process of impregnation. However, this case of fibre orientation does not reflect the real stacking sequence for wind turbine blades.

For the case shown in Fig. 28b, it has been found that when the fibres are orientated at $\theta=90^\circ$ (close to the practical case of design), the flow rate is slow compared with the previous case. This difference can be explained by the fact that when fibres are perpendicular to the direction of resin flow, the fibre arrangement will create a sort of barrier that prevents the resin from spreading easily in the fibrous medium because of the low presence of volume fraction of pores in such direction. Therefore, the idea of a concentric flow of resin with regard to the position of single-point injection is not truly representative for orthotropic fibre preforms.

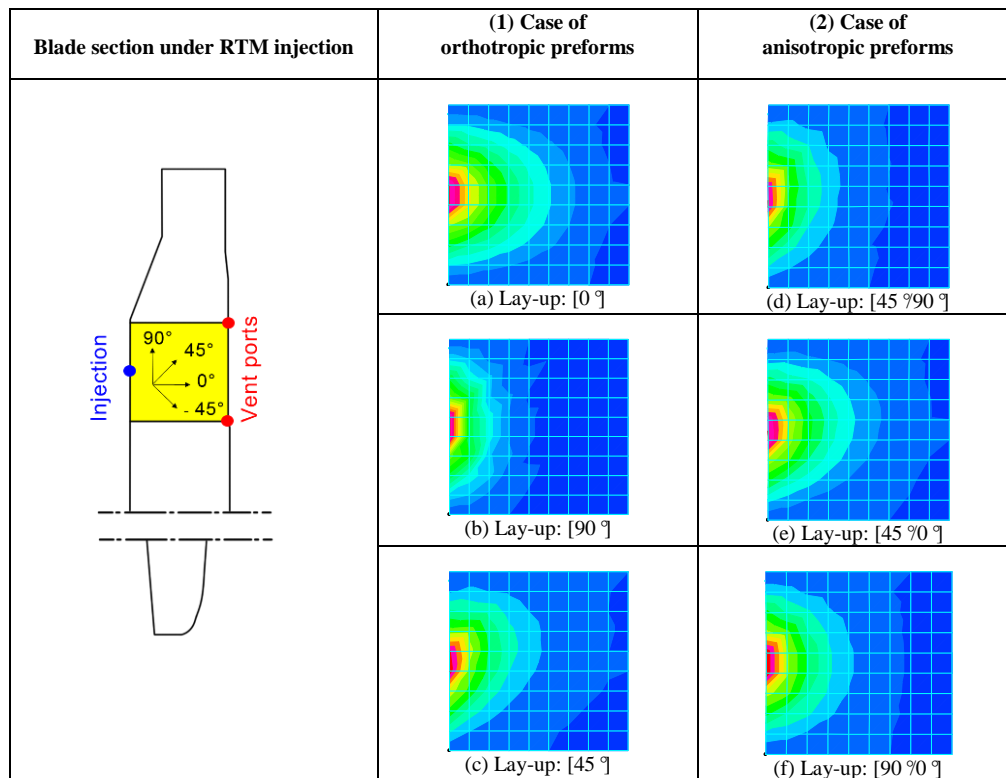


Fig. 28 Numerical simulation of resin flow behaviour during mould filling stage for one and double-layer fibrous preforms

2) Case of anisotropic preforms

For this case study, the positions of injection and vent ports are the same as those of the previous analysis. However, the three lay-up cases constituting the anisotropic preforms were achieved by superposing alternatively several unidirectional plies with two specific angles of fibre orientations. To this end, three different case studies were considered in this analysis; these are symbolised by the following stacking sequences: [45 °90 °], [45 °0 °] and [90 °0 °]. The output results of this investigation are presented in Fig. 28d-f.

It can be discerned that the resultant flow is dominant in the case where stacking arrangement presents a significant distribution of volume fraction pores through the fibrous preform. This provides a better flow of resin as shown in Fig. 28f. On the contrary, the drainage of resin is slower and less important for the case shown in Fig. 28d. In addition to the fibre direction effects, it should be pointed out that permeabilities depend also on the order of stacking sequence of layers (mainly for the transverse permeability). However, these factors were not considered in this analysis.

But, it should be noted that the choice of an appropriate stacking sequence is usually determined by a finite element structural analysis. The output results must meet the criteria required by the technical specifications and at the same time the applied standards for certification. Therefore, any change in the fibre orientation of layers constituting the preform may, in one hand, promote the process of drainage of the resin, but can, however, affect the mechanical properties of the material and consequently the stiffness and strength of the resulting composite wind turbine blade. The final choice of stacking sequence must respond favourably and simultaneously to the conditions defined by the numerical calculations and those imposed by the principles governing the RTM process. This particular issue should be carefully considered before the implementation of the RTM process.

V. REPAIR METHODS AND MAINTENANCE PROCEDURES

A. Different Types of Defects and Damage

1) Manufacturing defects or anomalies

Defects associated to composite wind turbine blades are usually due to the type of production process used and/or to the non-qualification of operators. In the ISO quality system, these defects are defined as “anomalies” that can be classified as either minor or major. Some of the anomalies that can appear during blade manufacturing are the following [32, 33]: improper fibre volume fraction, gel-coat/skin debonding, porosity; matrix cracking, misalignment of fibres, improper matrix distribution and so forth.

Poor impregnation between the plies and/or porosity defects may be the main factors that could cause the delamination

phenomenon. Its presence results in a separation between plies, and this can easily cause the risk of local buckling which could substantially alter the overall stiffness of the blade and its critical buckling load, and this can lead to premature failure of the blade. Therefore, a comprehensive study on the delamination growth must be performed on the most stressed upper and lower blade laminates, where the effects of the critical load on the length of delamination will be identified and analysed.

2) *Damage mechanisms*

Types of damage that may arise during service life can be classified as: bird strikes, harsh sun, lightning strikes, leading edge erosion (e.g., sand and sea-salt), surface erosion (e.g., heavy rain, ice, hail and insects), adhesive joint failure, gel-coat cracking, damage at the attachment points and material fatigue [33, 34].

According to the climatology of the region, offshore and onshore wind turbines are exposed to climatic conditions such as variations in temperature, moisture, sand and salt laden air. These natural events can easily damage the skin of the blade, especially the gel-coat layer. However, a composite wind turbine blade is highly durable if the layer that protects the blade skin from external environment exhibits good physico-chemical characteristics (e.g., high modulus of elasticity, good elongation after rupture, higher resistance to erosion, adequate thickness, absence of porosity, ..).

The inappropriate choice of these characteristics can result in risk of formation of blisters, creation of small cavities and appearance of cracks; resulting in a laminate exposure to external environment and facilitating contact with natural phenomena (e.g., ice, temperature variation, contact with sea/rain water, ..). These risks can be regarded as the main factors that accelerate degradation, aging and reduction of a wind turbine blade lifetime. Consequently, during the design process, a particular study on the behaviour of the gel-coat to weather events and to hygrothermomechanical loading must be undertaken to predict the adverse effects.

B. *Reference Documents for Repair*

Certifying bodies and associated documents for certification do not provide sufficient repair procedures specific for wind turbine blades. However, it is important that instructions for repair and maintenance must be clearly defined and standardized in order to be equitably exploited by the various wind energy companies. The availability of approved guidelines will regulate all activities related to the repair techniques and maintenance procedures for each type of composite wind turbine blade. Associated procedures should have the same level of requirements as the existing set of rules established by the FAA (Federal Aviation Administration) and DGCA (Directorate-General for Civil Aviation), namely the joint aviation requirements (i.e., JAR Part 145) and the federal aviation regulation (i.e., FAR Part 145).

C. *Repair Process*

Damages in service or manufacturing defects can be detected through periodic inspection or quality control, usually carried out by qualified operators. For manufacturing defects, the techniques that can be used for detecting the non-conformities include: visual inspection, tapping test or NDT (Non-Destructive Test). Moreover, for detecting damages in service, the most widely used techniques are mainly: thermography, shearography, binoculars, ultrasonic testing and sometimes X-Ray. However, it is recommended not to use the latter technology because of the potential risk of X-ray to human health.

According to the assessment of defects and damages (minor or major), the composite blade structure may be repaired or fully replaced using typical procedures, usually inspired from international aviation standards, for example the Aircraft Structural Repair Manual (SRM). For on-site repairs, operators must be qualified in repair of composite structures and in the same time have the climbing skills.

D. *Scarf Repair Technique*

The most common repair method used is the scarf repair method which is performed by the following steps (Fig. 29):

- localisation of the damaged area;
- removal of material at the damaged area;
- definition of the geometry of the area to be repaired;
- definition of the appropriate stacking sequence;
- cutting fibre plies with fitting sizes;
- application of an adhesive film;
- stacking up plies in accordance with the order and orientation assigned to each ply;
- adding extra plies (if this does not affect the aerodynamic efficiency of the blade);
- utilisation of hot bond repair unit for the curing phase (Fig. 30).

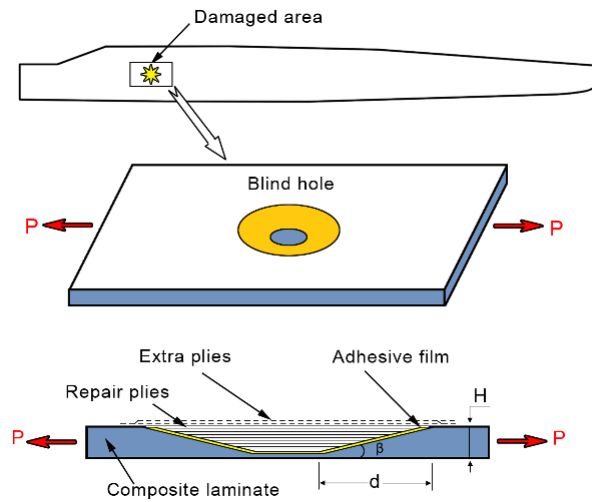


Fig. 29 Schematic showing the repair patch technique

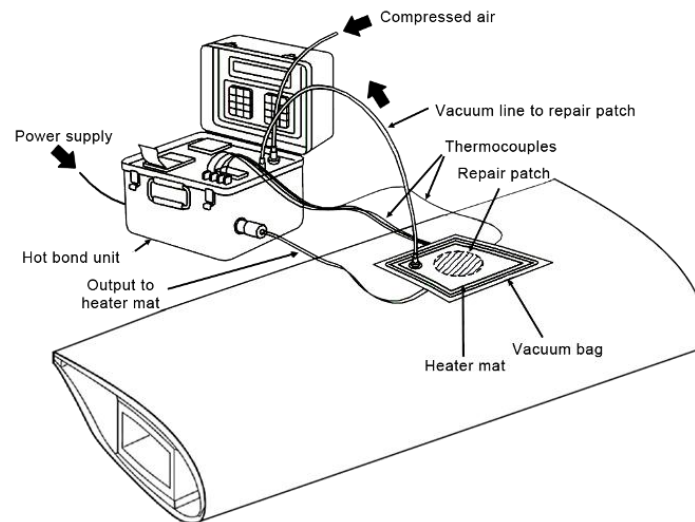


Fig. 30 On-site repair using a hot bond repair unit (Anita)

For instance, Fig. 29 shows the pattern of damage located near the transition zone. The damage is assumed to be a blind hole (30 to 80% of the thickness). The repair patch edges are tapered and the corresponding bevelled angle β is variable from 2 to 3. The filling operation is performed using the technique of deposition ply-by-ply or layer-by-layer. The necessary equipment for curing may be performed using a mobile hot bond repair unit, as shown in Fig. 30.

As the repaired structure will not have the same mechanical characteristics as the original one (undamaged structure), it is therefore important, but not indispensable, to add extra plies in order to compensate the loss in strength and stiffness. However, it should be noted that the added extra plies can create extra weight, and thus a residual unbalance (since the mass will not be uniformly distributed). On the other hand, extra plies may also cause stress concentration problem due to the slight modification in the blade aerodynamic profile at the repaired zone which may lead to a loss of skin smoothness and thereby reducing the aerodynamic efficiency of the blade.

VI. LIFE CYCLE ANALYSIS, ECODSIGN AND RECYCLING METHODS FOR COMPOSITE WIND TURBINE BLADES

A. Life Cycle Analysis of Composite Wind Turbine Blades

The life cycle analysis (LCA), or life cycle assessment, is an environmental evaluation method for quantifying the impacts of wind turbine blades throughout their entire life cycle, ranging from the extraction of raw materials, manufacturing, transportation, use and maintenance to the end of life, taking into account the sustainability requirements, REACH regulations and the ecodesign notion. Although the average lifespan of a composite wind turbine blade is between 20 to 25 years, it is predicted that by 2034, around 225000 tonnes of composite materials originated from wind turbine blades will be recycled each year all over the world.

International Standard ISO 14040 specifies and explains the different phases of the implementation of LCA before, during

and after the design process of composite wind turbine blades. From an environmental point of view, LCA plays a crucial role in developing effective ways to reduce ecological risks and help promote green production. With this in mind, environmentally conscious designers of blades have to factor in the impacts of their products on the environment and find new alternatives to make the blade-product more competitive in the worldwide composite market, by means of clear regulations, specific safety standards and legal predictability [12].

B. Ecodesign of Composite Wind Turbine Blades

In addition to the classical design criteria applied for the production of blades, the ecodesign notion is a new approach which takes into account new criteria for innovative blades, ranging from waste management, reduction in VOC emissions, optimisation of energy consumption, waste recovery system, to ways of recycling specific to blades retired from service. In order to achieve these requirements, an ecodesign key performance indicator (KPI) can be developed on the basis of probability theory rules. This KPI will provide blade designers the ability to control via green rules the performance level of assessment for each design step. For further details on this subject area, the reader is invited to refer to previous works conducted by the author and published elsewhere [36-38].

C. Recycling Methods for Composite Wind Turbine Blades

Composite materials used in the manufacture of wind turbine blades are a combination of fibres and a polymer matrix. The fibres chosen are usually glass fibres, carbon fibres, natural fibres or a hybrid (i.e., composed of two or more fibres of different natures). The polymer matrix selected may be thermosetting or thermoplastic. However, due to the existence of cross-linking phenomenon within the molecular chain of thermosetting polymer matrices, they are hard to recycle. Thus, there are actually two major recycling methods employed in the wind industry; these are: (i) the mechanical method and (ii) the thermal method.

For both recycling methods, the first step is to cut in-situ the retired wind turbine blades into small pieces in order to facilitate their transportation to the recycling plant. For the mechanical method, the following step is to crush with a mechanical hammer the blade pieces and transforming them into grains with variable diameters: e.g., 50 μm for fine grains and 10 mm for coarse grains. The recycled materials can then be used in other applications such as civil engineering. For the thermal method, the next step is to put (after the cutting operation) the different cut parts into a rotary kiln incinerator and then burn them at a temperature of 500 $^{\circ}\text{C}$ using the pyrolysis process. Consequently, the polymer matrix is fully burned and transformed into a gas which may be recovered and used for the production of electrical energy. Residues of the fibres can be used in other structural applications such as ingredients of concrete in the construction of buildings and roads. They can also be used as a structural component within other less stressed composite structures.

In fact, studies show that glass fibres are the most commonly used in the manufacture of wind turbine blades because they are less expensive. Whereas, thermosetting polymer matrices (polyester and epoxy) do not attract much the attention of blade manufacturers, as their use will face the problem of recyclability. In contrast, thermoplastic polymer matrix is one of the most attractive ones and is intended to be used in the manufacture of future wind turbine blades; it provides the possibility to be easily recycled after use and therefore sustainable. For instance, an innovative anionic polyamide PA-6 thermoplastic matrix has been developed and intended to be incorporated in the wind blade industry [39].

VII. PROCEDURES OF QUALIFICATION AND CERTIFICATION

A. Qualification of Wind Turbine Blades

This part includes static and dynamic testing of a composite wind blade manufactured by a special process. The qualification process is characterized by a verification of the compatibility between the blade design and the aerodynamic and/or environmental loads (temperature and moisture) that the blade may be subjected to during its lifetime. These tests consist in imposing a static and dynamic environment more severe than the real case [8].

The experimental testing methods consist in manufacturing a blade prototype and making it undergo static and dynamic testing in laboratory for the identification of critical areas that can cause failure. These experimental methods are described and detailed in Section III.

Working in this context, a test bench and strain gauges are needed to perform the fatigue testing. The experimental results will quantify the lifetime of the blade with a degree of confidence. On average, the lifespan is estimated at 23 years old.

B. Certification of Wind Turbine Blades

In accordance with ISO standards and IEC procedures relative to the blade design, Fig. 31 shows the main steps for the certification process [15]. Certification of wind blades may be issued by a competent body such as Germanischer Lloyd (GL).

The certification for a specific wind turbine blade is carried out on the basis of IEC 61400 standards and external audits which focus mainly on the following points:

- the evaluation of design reports and associated documents;

- the evaluation of the site and its manufacturing processes;
- the evaluation of testing equipment for static, dynamic and fatigue analyses;
- the control of the qualification of operators and workers involved in the design process;
- the evaluation of experimental/numerical results and validation of blade prototypes;
- the assessment of the quality management systems;
- the declaration of commitment regarding the periodic monitoring.

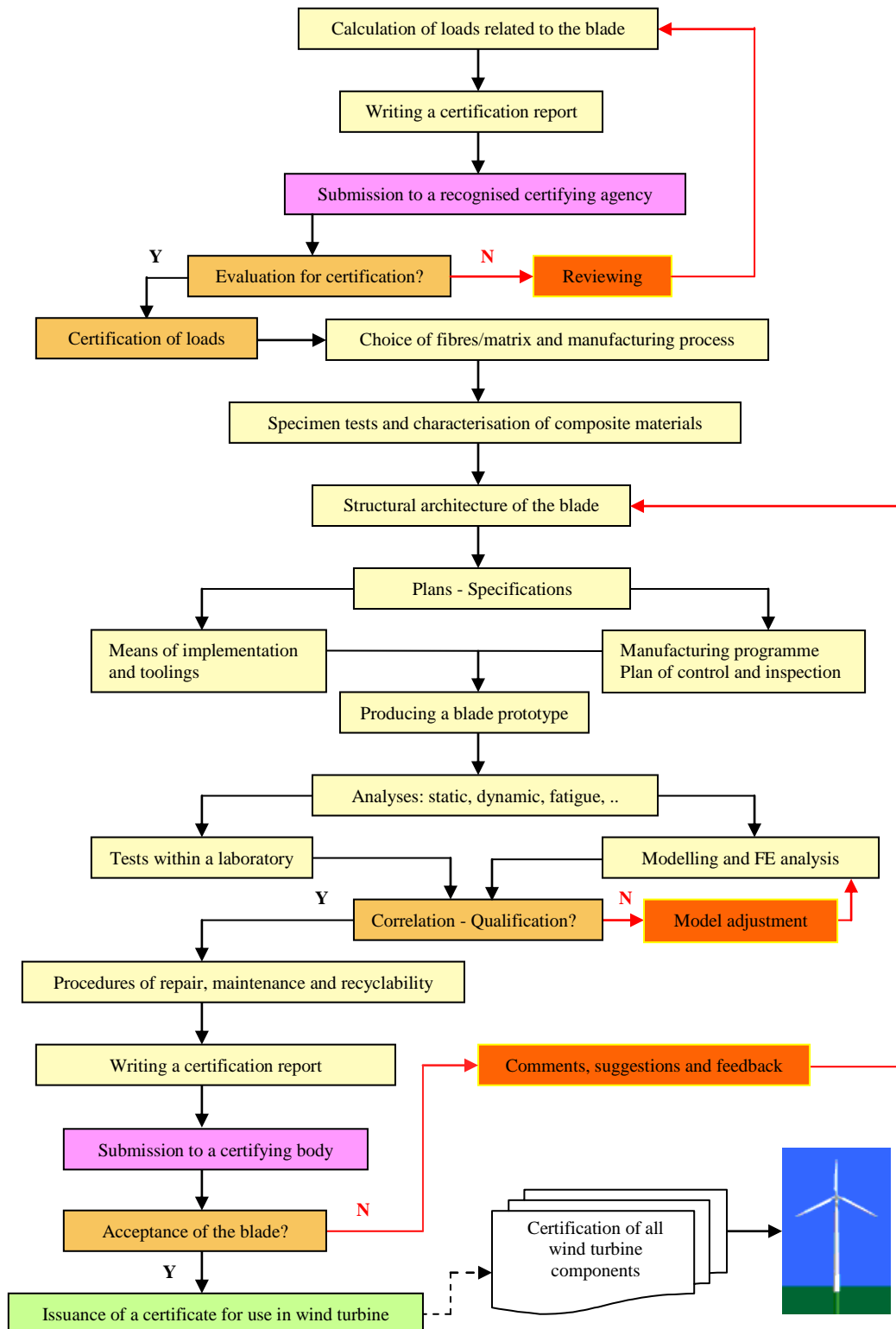


Fig. 31 Flowchart summarising the process of qualification/certification of a wind turbine blade

VIII. CONCLUSIONS

To minimise the effect of global warming and leave a more stable environment for future generations, each country with windy areas is encouraged to play a crucial role in boosting research, innovation and creativity in the field of wind energy, particularly in the technology of composite wind turbine blades. This eco-action can help energy consumers and stakeholders to be less dependent on the fossil fuels as the rate of GHG emissions is increasing and continue to accelerate the global warming phenomenon.

Moreover, this survey is in line with the European Union roadmap on wind energy and responds to the 3×20 objectives that must be achieved on 2020, namely:

- 20% reduction in GHG emissions;
- 20% increase in the share of renewable energies;
- 20% reduction in energy consumption.

For wind energy, composite materials based on glass fibres and/or carbon fibres occupy a predominant place in the modern industry of wind turbine blades. Indeed, these materials offer attractive advantages in terms of specific stiffness and specific strength. However, besides these advantages, the notion of ecodesign has to be taken into account in all design stages for the production of green, clean and eco-friendly wind turbine blades. As a matter of fact, the ecodesign approach has become one of the most efficient tools aiming to preserve the environment and protect human health during the design process and this, alongside traditional criteria such as cost effective, quality, feasibility and market expectations.

In fact, to meet the ecodesign requirements within the manufacturing processes of composite wind turbine blades, companies that are engaged towards the implementation of environmental management system (EMS) are encouraged to boost and develop the following main points:

- the development of clean manufacturing processes by reducing emissions of VOCs;
- the development of new high-performance materials with cost effective and environment friendly;
- the creation of specific standards for qualification, repair and recycling of composite blades at the end of their life-cycle;
- the implementation of cooperative activities between the university, research centres and the industry;
- the encouragement of innovative technology transfer;
- the development of university-entreprise training partnerships (UETPs) to form more technical engineers for production, repair and maintenance activities in the wind energy technology.

It is in the context of global efforts to fight against climate change for which this chapter has been developed enabling the improvement of design process, qualification and certification of future wind turbine blades. This will providentially offer great potential for the development of clean energy and the guarantee of a new security of energy supply. In addition, were also taken into account the environmental impacts and requirements regarding health, hygiene & safety, while remaining consistent with a logic cost-efficiency ratio.

ACKNOWLEDGMENT

The author would like to thank Mr. Cherif Attaf for his help and kind assistance in improving the quality of figures and illustrations which appear in this chapter.

REFERENCES

- [1] W. C. Wang, Y. L. Yung, A. A. Lacis, T. Mo, and J. E. Hansen, "Greenhouse effects due to man-made perturbations of trace gases," *Science*, vol. 194, iss. 4266, pp. 685-690, Nov. 1976.
- [2] W. D Nordhaus, "To slow or not to slow: the economics of the greenhouse effect," *The Economic Journal*, vol. 101, pp. 920-937, Jul. 1991.
- [3] "IPCC 1991: Report of the fifth session of the WMO/UNEP," Intergovernmental Panel on Climate Change (IPCC) 13-15 Mar. 1991, Geneva.
- [4] L. M. Kamp, R. E. H. M. Smits, C. D. Andreisse, "Notion on learning applied to wind turbine development in the Netherlands and Denmark," *Energy Policy*, vol. 32, iss. 14, pp. 1625-1637, Sept. 2004.
- [5] T. Justin, "New record: World's largest wind turbine (7+ Megawatts)," in News, Renewable Power, available on line at: <http://www.metaefficient.com/news/new-record-worlds-largest-wind-turbine-7-megawatts.html>, 2008.
- [6] A. Sarkar, D. K. Behera, "Wind turbine blade efficiency and power calculation with electrical analogy," *Int. Journal of Scientific and Research Publications*, vol. 2, iss. 2, Feb. 2012.
- [7] B. Attaf, and L. Holloway, "Vibrational analyses of glass reinforced polyester composite plates reinforced by a minimum mass central stiffener," *Composites*, vol. 21, N 5, 1990, p. 425-430.
- [8] B. Attaf, "Vibrational analyses of fibre-reinforced composite wind turbine blades: theory and experiment," *Europe's Premier Wind*

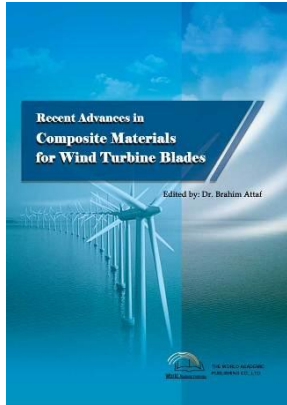
- Energy Event (EWEA 2013)*, paper ID 71, Vienna, 4-7 Feb. 2013.
- [9] J. Xu, and Z. Lu, "Application of fiber-reinforced composites in wind turbine blades," *World Non-Grid-Connected Wind Power and Energy Conference (WNWEC 2010)*, Nanjing, 5-7 Nov. 2010.
- [10] L. Hollaway, and B. Attaf, "On the vibration of glass/polyester composite stiffened and unstiffened rectangular plates," *Chinese Society of Aeronautics, in: Seventh International Conference on Composite Materials*, Beijing, 1989, p. 435-444.
- [11] J. Gou, F. Liang, Y. Tang, and J. Kapat, "Multifunctional nanocomposites for offshore wind energy," *Proc. of the 20th Int. Offshore & Polar Eng. Conf.*, Beijing, China, 20-25 Jun., 2010.
- [12] B. Attaf, "European eco-factor," *Pan European Networks: Science & Technology*, iss. 07, Jun. 2013, p. 128-129.
- [13] A. J. Hart, "Nanocomposites and fibers," Lectures/Tutorials - *University of Michigan*, ME599-002, Michigan, 15 Apr. 2009.
- [14] National Academy of Sciences report (2005), <http://www.nap.edu/catalog/11268>.
- [15] B. Attaf, "Eco-conception et développement des pales d'éoliennes en matériaux composites," *Revue des Energies Renouvelables - 1^{er} Séminaire Méditerranéen sur l'Energie Eolienne*, Tipasa, Algeria, 11-12 Apr., 2010, pp. 37-48.
- [16] B. Attaf, "Structural ecodesign of onshore and offshore composite wind turbine blades," *1^{ère} Conférence Franco-Syrienne sur les Energies Renouvelables*, 24-28 Oct., 2010, Damascus, Syria.
- [17] R. M. Jones, *Mechanics of composite materials*, Scripta Book Company, Washington, D.C., 1975.
- [18] O. Saarela, "Computer programs for mechanical analysis and design of polymer matrix composites," *Prog. Polym. Sci.*, vol. 19, pp. 171-201, 1994
- [19] T. Y. Yang, *Finite element structural analysis*, Prentice-Hall, Inc., New Jersey, 1986.
- [20] O. C. Zienkiewicz, R. L. Taylor, and J. Z. Zhu, *The finite element method: its bases and fundamentals*, Elsevier Butterworth-Heinemann, Oxford, 2005.
- [21] B. Attaf, "Vibration and stability analyses of unstiffened and stiffened composite plates," PhD thesis, University of Surrey, England, UK, Jun. 1990.
- [22] B. Attaf, and L. Hollaway, "Vibrational analyses of glass reinforced polyester composite plates reinforced by a minimum mass central stiffener," *Composites*, vol. 21, n 5, pp. 425-430, Sep. 1990.
- [23] B. Attaf, "Eco-bonding of composite wind turbine blade structural parts using eco-friendly adhesives," *Advances in Materials Science & Applications (AMSA)*, vol. 3, iss. 2, pp. 31-37, Jun. 2013.
- [24] K. M. Pillai, "Governing equations for unsaturated flow through woven fiber mats. Part 1. Isothermal flows," *Composites A*, vol. 33, no. 7, pp. 1007-1019, 2002.
- [25] C. Nardari, B. Ferret, and D. Gay, "Simultaneous engineering in design and manufacture using the RTM process," *Composites A*, vol. 33, no. 2, pp. 191-196, 2002.
- [26] B. Attaf, "Ecomoulding of composite wind turbine blades using green manufacturing RTM process," *ISRN Materials Science*, vol. 2012, Article ID 734328, 9 pages, 2012.
- [27] H. Darcy, *Les fontaines publiques de la ville de Dijon*, V. Dalmont, 1856, Paris.
- [28] A. Shojaei, S. R. Ghaffarian, and S. M. H Karimian, "Three-dimensional process cycle simulation of composite parts manufactured by resin transfer molding," *Compos Struct* 65, pp. 381-390, 2004.
- [29] H. Kris et al., "New set-up for measurement of permeability properties of fibrous reinforcements for RTM," *Composites: Part A* 33, pp. 959-969, 2002.
- [30] H. P. Chung, I. L. Woo, S. H. Woo, and A. Vautrin, "Weight minimization of composite laminated plates with multiple constraints," *Compos Sci Technol* (63), pp. 1015-1026, 2003.
- [31] H. Jinlian, L. Yi, and S. Xueming, "Study on void formation in multi-layer woven fabrics," *Composites: Part A* 35, pp. 595-603, 2004.
- [32] M. Gower, G. Sims, R. Lee, S. Frost, and M. Wall, "Assessment and criticality of defects and damage in Material systems," Measurement Good Practice Guide No. 78, National Physical Laboratory, Teddington, Middlesex, UK, Jun. 2005.
- [33] E. Greene, *Marine Composites NDE: Wind Energy*, SSC Project SR-1464, pp. 54-59.
- [34] G. Marsh, "Meeting the challenge of wind turbine repair," *Reinforced Plastics*, pp. 32-36, Jul. /Aug. 2011.
- [35] K. Larsen, "Recycling wind turbine blades," *Renewable Energy Focus*, 2009.
- [36] B. Attaf, "Generation of new eco-friendly composite materials via the integration of ecodesign coefficients," In Brahim Attaf (ed.), *Advances in composite materials-Ecodesign and analysis*. Intech Open Access Publisher, 2011, p. 1-20.
- [37] B. Attaf, "Probability approach in ecodesign of fibre-reinforced composite structures," in *Proc. CAM'09*, Algeria, 2009.
- [38] B. Attaf, "Eco-characterisation of composite materials," *JEC Composites* 42, 2008, p. 58-60.
- [39] K. V. Rijswijk, "Thermoplastic Composite Wind Turbine Blades – Vacuum Infusion Technology for Anionic Polyamide-6 Composites," PhD dissertation, Delft University of Technology, Delft, 2007.

Brahim Attaf works as an independent Expert/Researcher in the field of composite materials and structures. He obtained his Engineering degree from the Ecole Nationale Polytechnique of Algiers (ENPA), Algiers, Algeria, in 1985, and then his Ph.D. degree from the University of Surrey, Guildford, UK, in 1990.

He has previously worked as a Lecturer/Researcher (Maitre de Conférences) within the Departments of Aeronautics, Mechanics and Civil Engineering at the University of Blida in Algeria (1990–2000), and he was responsible for design office and quality assurance with composite firms in France (2000–2003). Since 2003 he has been independently involved in sustainability research actions leading to ecodesign of composite materials and structures through the integration of environmental and health aspects into product lifecycle. His main

research and teaching interests focus on vibration and stability analyses of composite structures subjected to hygrothermomechanical loading using finite-element approach and experimental investigations.

Dr. Attaf has published many scientific papers, edited two books, and successfully trained/supervised many engineers and postgraduate students (Master's and Ph.D.'s).



Recent Advances in Composite Materials for Wind Turbine Blades

Edited by Dr. Brahim Attaf

ISBN 978-0-9889190-0-6

Hard cover, 232 pages

Publisher: The World Academic Publishing Co. Ltd.

Published in printed edition: 20, December 2013

Published online: 20, December 2013

This book of science and technology provides an overview of recent research activities on the application of fibre-reinforced composite materials used in wind turbine blades. Great emphasis was given to the work of scientists, researchers and industrialists who are active in the field and to the latest developments achieved in new materials, manufacturing processes, architectures, aerodynamics, optimum design, testing techniques, etc.. These innovative topics will open up great perspectives for the development of large scale blades for on- and off-shore applications. In addition, the variety of the presented chapters will offer readers access to global studies of research & innovation, technology transfer and dissemination of results and will respond effectively to issues related to improving the energy efficiency strategy for 2020 and the longer term.

How to cite this book chapter

Attaf, B. (2013). Designing Composite Wind Turbine Blades from Cradle to Cradle, *Recent Advances in Composite Materials for Wind Turbines Blades*, Dr. Brahim Attaf (Ed.), ISBN 978-0-9889190-0-6, WAP-AMSA, Available from: <http://www.academicpub.org/amsa/chapterInfo.aspx>

World Academic Publishing - Advances in Materials Science and Applications

